TECHNICAL MEMORANDUMS

NATIONAL ADVISORY COMMITTEE FOR AERONAUTICS

No. 679

EXPERIMENTAL DETERMINATION OF THE THICKNESS OF THE BOUNDARY LAYER ALONG A WING SECTION

By Otto Cuno

Zeitschrift für Flugtechnik und Motorluftschiffahrt
Vol. 23, No. 7, April 14, 1932
Verlag von R. Oldenbourg, München und Berlin

Washington
August, 1932

NATIONAL ADVISORY COMMITTEE FOR AERONAUTICS

TECHNICAL MEMORANDUM NO. 679

EXPERIMENTAL DETERMINATION OF THE THICKNESS OF THE BOUNDARY LAYER ALONG A WING SECTION*

By Otto Cuno

The thickness and course of the boundary layer were measured in flight, in order to determine whether the relations on an airplane and on a shop-made wing can be brought into agreement with the results of wind-tunnel tests and Horst Müller's calculations of the thickness of the boundary layer, as developed from Karman's integral equation for the boundary layer.

The boundary layer plays an important part in the improvement of airplane wings. It can be reduced by improving the shape of the wing. Reducing the boundary layer by suction or other means makes it possible to obtain better profile characteristics. Before considering these innovations, however, an accurate knowledge of the velocity distribution, boundary-layer thickness and separation points is essential.

In order to determine the relative velocities along a wing section, a set of total-head tubes was used, as shown in Figure 1. Its support was so constructed that the whole set could be moved along a wing section. A wind-tunnel test showed that the tubes did not appreciably affect one another. Each pressure tube was connected with a manometer by a copper tube with a multiple cock. The whole series of tests was flown under constant conditions of engine speed, angle of attack and flight speed. Ten test stations were selected along the wing chord and ten test points were taken along the normal to the wing surface at each station. (See fig. 1, top.) Each pressure tube could be separately connected with the manometer by means of the multiple cock. The test flights were made with a Klemm L 26 II a airplane.

---

*"Experimentelle Untersuchung der Grenzschichtdicke und Verlauf längs eines Flügelschnittes." Zeitschrift für Flugtechnik und Motorluftschiffahrt, April 14, 1932, pp. 189-191.

TEST DATA

Rated engine power	80 hp
Power during test	65 "
Engine speed during test	1,600 r.p.m.
Angle of attack	1 degree
Flight speed	122 km/h
Time required for manometer water column to come to rest	50 seconds
Distance of test section from center of fuselage	2.2 meters

NOTATION

p_o (kg/m²), static pressure in undisturbed flow.

q_o " dynamic " " " "

p_1 " static pressure at test station.

q_1 " dynamic " " " " outside of boundary layer.

y (mm), distance of test point from surface of wing.

p_s (kg/m²), pressure difference in seat at open end of manometer.

δ (mm), thickness of boundary layer.

z " manometer deflection.

l " developed contour of top of profile.

s " developed contour from leading edge to test station.

u (m/s), velocity outside of boundary layer.

U (m/s), " inside " " "

The manometer shows the pressure head as the total energy

$$z\,\gamma_{water} = p + q \qquad (1)$$

Any variation of this value z across the boundary layer indicates a corresponding variation in the total energy. Figure 2 shows that the energy curve in the boundary layer increases from zero to a constant value. This curve is identical, however, with the velocity drop in the boundary layer, since the pressure p is constant in the region over the test station. Outside of the boundary layer, the z values are everywhere constant, while they decrease in the boundary layer, indicating a loss of energy.

The z value characterized by the manometer reading indicates

$$z\,\gamma_w = p_1 + q_1 - p_s \qquad (2)$$

The pressure difference p_s at the open end of the manometer was determined by means of a Pitot tube, by first connecting the manometer with the total-head lead only and then with both the total-head and static leads of the same instrument. The difference between the two readings is p_s.

From equation (2), we obtain the value of the velocity for

$$q_1 = \gamma_l \frac{u^2}{2g} = z\,\gamma_w - p_1 + p_s \qquad (3)$$

The still unknown pressure p_1 is calculated from the velocity distribution around the profile. The velocity is measured at every test station by means of a Pitot tube, and well outside the boundary layer, at a distance of 12 cm (4.72 in.) from the wing. Since the energy is everywhere the same outside the boundary layer, we have

$$p_o + q_o = p_1 + q_1 \qquad (4)$$

whence

$$p_1 = p_o + q_o - q_1 \qquad (5)$$

The resulting values are plotted in Figure 3 and give the velocity distribution. Both positive and negative pressures are indicated.

Figure 2 shows the velocity distribution in the boundary layer on the upper side of the wing, as obtained from the tests. The distance y of the test point from the wing is plotted on the ordinate. The developed contour of the profile with its test points is plotted on the abscissa, as also the velocity head starting from the test point in question. From the curve diagram it is obvious that the velocity variation toward the leading edge is limited to a much smaller y range. The curves of the relative speeds flatten out with decreasing s/l, that is, toward the trailing edge. The dash-dot curve δ characterizes the boundary-layer thickness, which may be represented by making its ordinate equal to the distance of the contact point of the first vertical tangent from the axis of the abscissas. The boundary-layer thickness increases ever more rapidly from 4 mm (0.16 in.) at the leading edge to 60 mm (2.36 in.) at the trailing edge.

Figure 4 shows the velocity ratios in the boundary layer. The curves represent equal current velocities in terms of the corresponding heights. They are plotted for the velocity ratios:

$$\frac{U}{u} = 1; \quad \frac{U}{u} = 0.9; \quad \frac{U}{u} = 0.85; \quad \frac{U}{u} = 0.7; \quad \frac{U}{u} = 0.5$$

where U denotes the velocity in the boundary layer and u the velocity of the outer undisturbed flow.

The great divergence of the curves is apparently due to the unevenness of the shop-made airfoil and to disturbances resulting from imperfect transition between fabric and wood covering. During the tests it was found that the profile of a wing in flight does not remain perfectly constant. It was also found that, at the trailing edge of the airfoil where the pressure is positive on both sides, the fabric covering is pressed in as much as 5 mm (0.2 in.) on both sides, thus making the trailing edge 10 mm (0.4 in.) thinner than that of the adopted profile.

The measured boundary-layer thickness on the lower side of the airfoil is represented in Figure 5. It increases almost uniformly from 3 mm (0.12 in.) at the lead-

ing edge to 12 mm (0.47 in.) at the trailing edge. The discrepancy in the two boundary-layer curves is due to the great difference in the pressure distribution on the upper and lower sides of the airfoil.

CALCULATION OF THE BOUNDARY-LAYER THICKNESS FROM THE VELOCITY DISTRIBUTION

In order to compare the theoretical and experimental results, the boundary-layer thickness δ was calculated as suggested by Horst Müller.* From Karman's integral equation for the boundary layer its thickness was found by

$$\left(\frac{\delta}{l}\right)^{1-m} = -\frac{G}{B} R_l^m \lambda^{\frac{A}{B}} \int_0^{s/l} \lambda^{\frac{m}{2}-\frac{A}{B}} d\left(\frac{s}{l}\right) \qquad (6)$$

In which

s = developed contour of profile from the forward stagnation point.

l = length of total profile development.

δ = thickness of boundary layer.

n = 1/7 power exponent.

m = - 1/4 power exponent.

λ = q/q_0.

A = 115/576, constant according to Horst Müller.

B = - 7/72, " " " " "

G = 0.00281, " " " " "

*"Der Reibungswiderstand umströmter Körper." Werft-Reederei-Hafen No. 4, 1932, pp. 54-56.

Then

$$\left(\frac{\delta}{l}\right)^{5/4} = 0.289\ R_l^{-1/4}\ \lambda^{-2.055} \int_0^{s/l} \lambda^{1.93}\ d\left(\frac{s}{l}\right) \qquad (7)$$

in which

$$R_l = \frac{v_o\, l}{\nu} = 4500000$$

$$l = 1.85 \text{ m}$$

$$v_o = 32 \text{ m/s}$$

$$\nu = 1.35 \times 10^{-5} \text{ m}^2/\text{s}$$

The resulting partial equation

$$H = \lambda^{-2.055} \int_0^{s/l} \lambda^{1.93}\ d\left(\frac{s}{l}\right) \qquad (8)$$

was graphically evaluated, yielding the H curve. Further

$$\left(\frac{\delta}{l}\right)^{5/4} = 0.0063\ H \qquad (9)$$

and finally

$$\delta = \left(\sqrt[4]{0.0063\ H}\right)^5 l \qquad (10)$$

In Figure 6 the boundary-layer thicknesses are plotted against s/l. Curve 1 represents the experimentally determined thickness, while curve 2 represents the theoretical thickness. They practically coincide up to 70 per cent of the profile chord, from which point there is a pronounced separation. It is therefore assumed that the boundary-layer thickness is greatly affected by the increasing vortex formation at the trailing edge of the airfoil, thus causing the great discrepancy between the actual and the theoretical thickness.

CONCLUSIONS

The flight tests showed that the course of the boundary-layer thickness thus determined agrees with the wind-tunnel data and with the theoretical data from the velocity distribution. In the region of increasing vortex formation at the trailing edge of the wing, the thickness of the boundary layer increases more rapidly according to the tests than according to the calculation. The experimental apparatus worked well in every respect and yielded rapid and accurate measurements.

Translation by Dwight M. Miner,
National Advisory Committee
for Aeronautics.

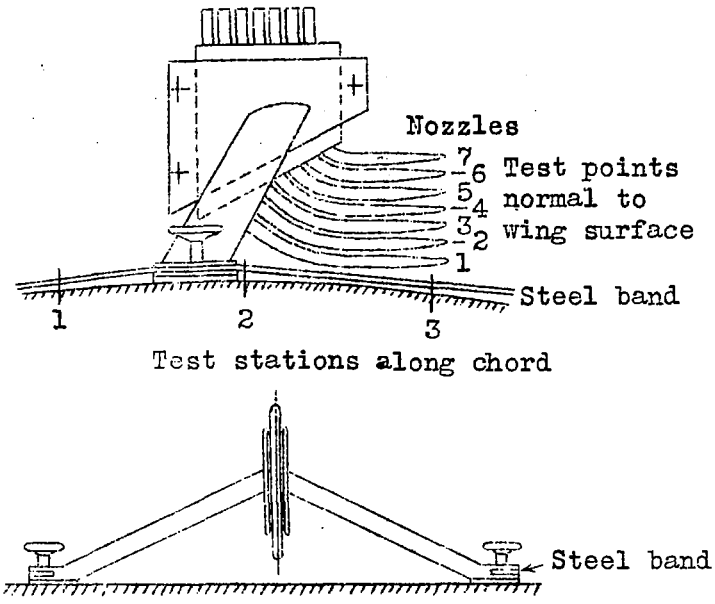

Fig. 1 Apparatus

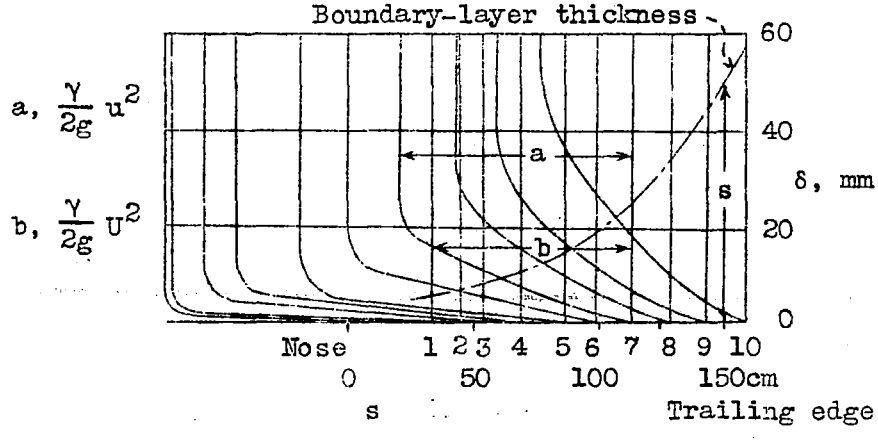

Fig. 2 Velocity curves and boundary-layer thickness.

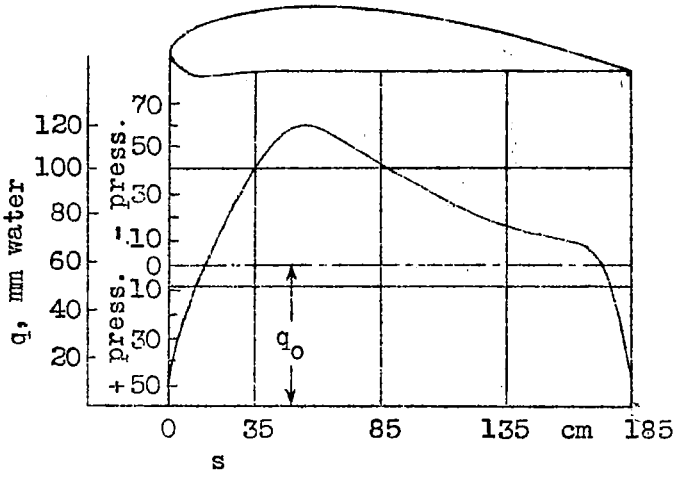

Fig. 3 Pressure distribution on upper side of wing.

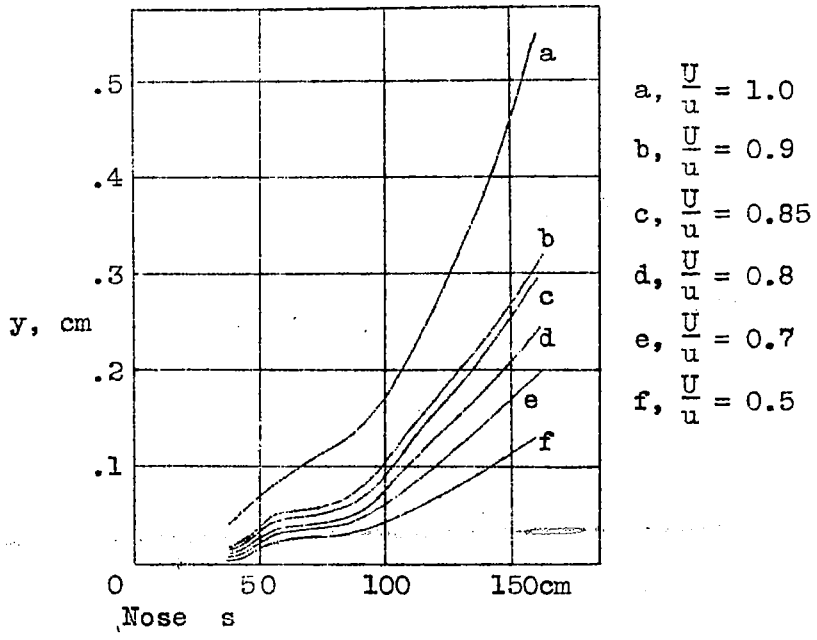

Fig. 4 Velocity distribution in boundary layer.

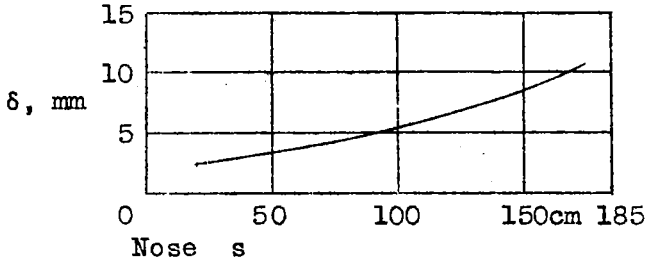

Fig. 5 Thickness of boundary layer on lower side of wing.

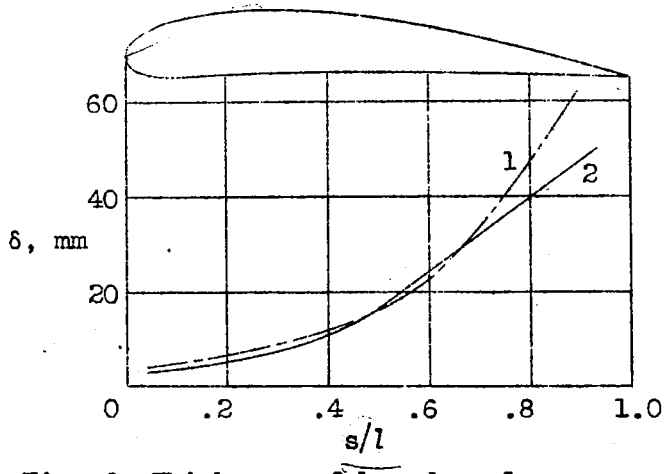

Fig. 6 Thickness of boundary layer on upper side of wing.